Author Manuscript
Author Manuscript
Author Manuscript

HHS Public Access

Author manuscript

*Cell Rep*. Author manuscript; available in PMC 2016 January 16.

Published in final edited form as:

*Cell Rep*. 2016 January 12; 14(2): 200–207. doi:10.1016/j.celrep.2015.12.022.

# DGKθ Catalytic Activity is Required for Efficient Recycling of Presynaptic Vesicles at Excitatory Synapses

**Hana L. Goldschmidt**[1], **Becky Tu-Sekine**[1], **Lenora Volk**[2], **Victor Anggono**[3], **Richard L. Huganir**[2,§], and **Daniel M. Raben**[1,§]

[1]Department of Biological Chemistry, Johns Hopkins School of Medicine, Hunterian 503, 725 N. Wolfe St, Baltimore, MD 21205, USA

[2]Department of Neuroscience and Howard Hughes Medical Institute, Johns Hopkins University School of Medicine, Hunterian 1001, 725 N. Wolfe Street, Baltimore, MD 21205, USA

[3]Clem Jones Centre for Ageing Dementia Research, Queensland Brain Institute, The University of Queensland, Brisbane, QLD 4072, Australia

## Summary

Synaptic transmission relies on coordinated coupling of synaptic vesicle (SV) exocytosis and endocytosis. While much attention has focused on characterizing proteins involved in SV recycling, the roles of membrane lipids and their metabolism remain poorly understood. Diacylglycerol, a major signaling lipid produced at synapses during synaptic transmission, is regulated by diacylglycerol kinase (DGK). Here we report a role for DGKθ in the mammalian central nervous system in facilitating recycling of presynaptic vesicles at excitatory synapses. Using synaptophysin- and vGlut1-pHluorin optical reporters, we found that acute and chronic deletion of DGKθ attenuated the recovery of SVs following neuronal stimulation. Rescue of recycling kinetics required DGKθ kinase activity. Our data establish a role for DGK catalytic activity and its byproduct, phosphatidic acid, at the presynaptic nerve terminal in SV recycling. Together these data suggest DGKθ supports synaptic transmission during periods of elevated neuronal activity.

## Introduction

Efficient communication between neurons is essential for proper brain function. This process is triggered by $Ca^{2+}$-influx into presynaptic nerve terminals, resulting in fusion of synaptic vesicles (SVs) with the plasma membrane (exocytosis) and release of neurotransmitters into the synaptic cleft. A typical nerve terminal contains a relatively small number of vesicles, enough to maintain about 5–10 seconds of neurotransmission. Thus after

§Correspondence: The Johns Hopkins School of Medicine, Department of Biological Chemistry, Hunterian Bldg. 503, 725 N. Wolfe St., Baltimore, MD 21205, USA, Phone: 410-955-1289, draben@jhmi.edu. The Johns Hopkins School of Medicine, Department of Neuroscience and Howard Hughes Medical Institute, Hunterian Bldg. 1001, 725 N. Wolfe St., Baltimore, MD 21205, USA, Phone: 410-955-4050, rhuganir@jhmi.edu.

exocytosis, SVs must be retrieved and recycled by endocytosis in order to maintain synaptic transmission (Südhof, 2004). This becomes particularly critical during periods of elevated neuronal activity, where multiple SVs undergo exocytosis over a short period of time (Cheung et al., 2010). SV recycling is therefore essential for neuronal function, and its dysregulation may contribute to several neurological and psychiatric disorders (Kavalali, 2006).

Despite being a well-studied cellular process, the mechanisms that mediate the steps of the SV cycle, particularly those involved in endocytosis, remain a matter of debate. To date, four mechanisms of SV endocytosis have been described: (1) clathrin-mediated endocytosis (CME), (2) activity-dependent bulk endocytosis (ADBE) (Cheung et al., 2010), (3) kiss-and-run (Südhof, 2004), and (4) ultra-fast-endocytosis (Watanabe et al., 2013). These pathways are differentially utilized depending on the strength and duration of neuronal activity, as well as differ in their molecular machinery, speed and capacity for membrane retrieval (Clayton and Cousin, 2009; Kononenko and Haucke, 2015; Südhof, 2004; Watanabe et al., 2013; Wu et al., 2014).

Numerous proteins regulate SV endocytosis in mammalian central neurons (Haucke et al., 2011). Equally important, the lipid composition of the presynaptic membrane plays an active role in this process. Of the membrane lipids studied so far, phosphoinositides have the most well established role in SV endocytosis (Puchkov and Haucke, 2013; Rohrbough and Broadie, 2005). Phosphatidylinositol-4,5-bisphosphate (PtdIns(4,5)$P_2$) modulates SV recycling by recruiting and activating key molecules, such as synaptotagmin I (Chapman, 2008), clathrin adaptor protein AP2 and dynamin-1 (Burger et al., 2000; Di Paolo et al., 2004) to the presynaptic membrane. Genetic deletions of the lipid kinase (phosphatidylinositol phosphate kinase type Iγ, PIPK1γ) (Di Paolo et al., 2004), or the lipid phosphatase (synaptojanin 1) (Cremona et al., 1999; Mani et al., 2007) that mediate the generation and metabolism of PtdIns(4,5)$P_2$ respectively, result in multiple synaptic defects, including impaired SV recycling. PtdIns(4,5)$P_2$ is also a substrate for phospholipase C, which produces the signaling lipid, diacylglycerol (DAG).

DAG has been implicated in synaptic function and may play at least three roles in the SV cycle (Tu-Sekine and Raben, 2011). First, DAG enhances the activity of Munc13-1, which mediates the priming of SVs, a crucial step in SV exocytosis during spontaneous and evoked synaptic transmission (Augustin et al., 1999; Bauer et al., 2007). Second, DAG activates protein kinase C (PKC), which phosphorylates and thereby regulates the activities of presynaptic SNARE complex proteins, including Munc-18 and SNAP-25 (Di Paolo et al., 2004; Rhee et al., 2002). Finally, termination of DAG signaling through its phosphorylation by DAG kinases (DGKs) results in the production of phosphatidic acid (PtdOH), an acidic phospholipid which is also a signaling molecule as well as a precursor for the generation of PtdIns(4,5)$P_2$ (Antonescu et al., 2010; Luo et al., 2004).

Despite the importance of DAG and PtdOH in SV recycling, not much is known regarding the role of DGKs in SV recycling and presynaptic function. Understanding their roles is complicated by the fact there are ten mammalian DGK isoforms (α, β, γ, δ, ε, ζ, η, θ, ι, κ), all of which posses the same catalytic activity, are expressed in the CNS, and nine of them are found in neurons (Mérida et al., 2008; Tu-Sekine and Raben, 2011). Several functional studies have implicated individual DGK isoforms (β, ζ, ε, η) in modulating spine dynamics, neuronal plasticity and neurological disorders (Kakefuda et al., 2010; Kim et al., 2010; Musto and Bazan, 2006; Shirai et al., 2010). The roles of other DGKs localized to the presynaptic terminal are less well understood. Indeed, DGKι is the only isoform that has been implicated in presynaptic release (Yang et al., 2011). The notion that this family of enzymes might play a role in regulating SV recycling is supported by studies in *C. elegans* which found that DGK-1 activity suppresses acetylcholine release from the neuromuscular junction (McMullan et al., 2006; Nurrish et al., 1999). The ortholog of DGK-1 in mammals is DGKθ, the only type V DGK and whose function has never been described in the nervous system.

Here, we report that DGKθ plays an important role in modulating SV recycling in mammalian central neurons. Both shRNA-mediated knockdown of DGKθ and neurons derived from DGKθ knock-out mice exhibit a decreased rate of SV endocytosis compared to wild-type neurons. Importantly, this defect can be rescued by ectopic expressions of enzymatically active, but not a kinase-dead DGKθ. Our data establish a role for DGKθ kinase activity in the regulation of SV recycling, and suggest that DGKθ supports synaptic transmission during periods of sustained neuronal activity.

## Results

### DGKθ localizes to excitatory synapses in the mouse forebrain

DGKθ expression has been detected in multiple regions of the late embryonic (Ueda et al., 2013) and adult mouse brain (Houssa et al., 1997; Tu-Sekine and Raben, 2011), albeit at low cellular and temporal resolution. In order to study the role of DGKθ in brain function, we first examined DGKθ expression across multiple brain regions in adult mice. Western blot analysis using an isoform-specific antibody that recognizes the c-terminal region of DGKθ revealed a wide-spread expression of DGKθ in all brain regions examined, including the cortex and hippocampus (Figure 1A), consistent with the previously reported mRNA expression pattern (Houssa et al., 1997). DGKθ was detected in the forebrain, but not in the cultured glial cells prepared from the same brain region (Figure 1B), indicating a specific expression of DGKθ in neuronal cells. The expression of DGKθ was up-regulated during development, which peaked at postnatal day 14 (P14), coincident with the expression of synaptophysin, an integral SV protein with an established function at synapses (Figure 1C). A similar increase in DGKθ protein during synapse formation and development was also observed in cultured neurons (DIV 7–14, data not shown). Subcellular fractionation analysis of an adult mouse brain showed a general distribution of DGKθ in the cytosolic, microsomal and synaptosomal fractions (Figure 1D). DGKθ was also detected in the post-synaptic density fraction, albeit at a lower level, suggesting its presence at both pre- and postsynaptic sites.

To verify the biochemical results we examined endogenous DGKθ localization by immunofluorescence microscopy. Consistent with fractionation experiments DGKθ was detected throughout the neuron, including the soma, MAP2-positive dendrites, and MAP2-negative axons (Figures 1E–1F). Strikingly we found that DGKθ had a punctate distribution along dendrites which significantly overlaps with the excitatory presynaptic protein vGlut1 (Figures 1E–1F). Quantification of the overlap between these two signals showed that 62.6±1.4% of DGKθ overlapped with vGlut1 and 56.6±1.5% of vGlut1 overlapped with DGKθ per μm of dendrite (Figure 1G). In contrast, only 10.0±0.7% of DGKθ overlapped with the inhibitory presynaptic protein VGAT per μm of dendrite (Figures 1F–1G), suggesting that DGKθ preferentially localizes to excitatory synapses.

## Knockdown of DGKθ slows the rate of synaptic vesicle recycling

DGKθ localization to excitatory synapses and the onset of its expression during synaptogenesis suggested a potential role for this enzyme in excitatory synaptic transmission. Given the role of the DGKθ ortholog in *C. elegans* (McMullan et al., 2006; Nurrish et al., 1999), we predicted that DGKθ might posses a similar synaptic function at the presynaptic terminal. To test this, we generated a short-hairpin RNA construct directed against endogenous DGKθ mRNA (Figure 2A) to suppress DGKθ protein expression. Western blot analysis showed that lentiviral-mediated expression of DGKθ-shRNA in cortical neurons resulted in >90% knockdown of DGKθ protein compared to control shRNA-infected cells (Figure 2B).

To determine the effect of reduced DGKθ protein levels on presynaptic function, we used the pH-sensitive optical reporter synaptophysin-pHluorin (sypHy (Granseth et al., 2006)) to monitor SV recycling dynamics. Cortical neurons were co-transfected with sypHy and DGKθ-shRNA or a control shRNA, and allowed to express for 48 hours prior to measuring SV recycling kinetics. Knockdown of DGKθ significantly slowed the rate of SV endocytosis following KCl-induced neuronal depolarization compared to control neurons (Figures 2C–2D, $\tau$ = 59.2±4.2 s and 32.4±1.9 s, respectively). Moreover, expression of shRNA-resistant human DGKθ ($^{myc}$DGKθ) was sufficient to rescue the observed defect in endocytosis in neurons expressing DGKθ-shRNA, thus verifying the specificity of DGKθ-shRNA in our study (Figure 2D, $\tau$ = 34.9±4 s). Importantly, similar results were obtained when neurons were stimulated with a train of 300 action potentials (APs, 10Hz), supporting the role of DGKθ in regulating SV recycling in central neurons (Figures 2E–2F, **S1A**). To confirm that the effect of DGKθ-knockdown was not due to a specific defect in the sorting of a particular SV protein (synaptophysin in this case), we measured SV recycling kinetics using a different pHluorin reporter, vGlut1-pHluorin (vGlut1-pH, (Balaji and Ryan, 2007)). Consistent with the sypHy data, the kinetics of vGlut1-pH recycling following a train of 300 APs (10Hz) were also significantly slower in DGKθ-shRNA expressing neurons compared to controls (Figure S1B). Together, these data indicate that DGKθ is involved in the general retrieval mechanism of SVs, rather than regulating the sorting of a specific SV protein.

Since the strength of the stimulus can activate distinct recycling mechanisms (Clayton and Cousin, 2009; Kononenko and Haucke, 2015), we speculated that elevated neuronal activity may exaggerate the defect in SV recycling observed in DGKθ-knockdown neurons. As shown in Figures S1B–S1C, the delay in endocytosis kinetics of sypHy or vGlut1-pH in DGKθ knockdown neurons was larger when stimulated with trains of 600 APs (50Hz) compared to 300 APs (10Hz). Furthermore, a relatively smaller, but significant, delay in the rate of endocytosis was also observed when neurons were stimulated with a train of 40 APs

(20Hz), which is known to mobilize primarily the readily releasable pool of SVs (Burrone et al., 2006) (Figure S1D). Taken together, these data demonstrate that DGKθ is crucial for maintaining efficient recycling of SVs via distinct pathways of membrane retrieval in a use-dependent manner.

### DGKθ knock-out mice have a reduced DGK activity in the brain and exhibited impaired SV recycling efficiency

Next, we investigated the role of DGKθ with the use of a DGKθ homozygous knock-out (KO) mouse (see methods, Figure 3A). The genotypes and the levels of DGKθ protein expression in wild-type (WT), heterozygous (Het) and KO mice were confirmed by PCR and western blotting analyses, respectively (Figures 3A–3B). DGKθ KO mice appeared overtly healthy and did not display any obvious gross morphological differences in body size, mating, and lifespan compared to WT mice (data not shown). In addition, we did not observe any compensatory increase in other neuronal DGK isoforms, all of which are capable of catalyzing the production of PtdOH, in the brain of DGKθ KO mouse (Figure 3C). Surprisingly, we detected a significant decrease in total DGK activity measured in protein extracts from adult KO forebrain compared to WT (Figure 3D, Tu-Sekine and Raben, 2012). These data support a role for DGKθ in the production of PtdOH in the brain.

To confirm the role of DGKθ in regulating the kinetics of SV recycling, we measured the efficiency of sypHy retrieval in neurons derived from WT and DGKθ KO mice. Consistent with our previous results, the rate of endocytosis was significantly slower in KO neurons following a train of 600 APs compared to WT controls (Figures 4A–4B, $\tau$WT = 27.9±0.8 s vs $\tau$KO = 60.2±1.1 s). The endocytic defect in KO neurons was accompanied by a significant increase in sypHy fluorescence intensity 200 s post-stimulation (Figure S2B), indicating the accumulation of SV proteins on the cell surface. We also ruled out the role of DGKθ in regulating SV exocytosis in neurons (Figures S2C–S2E). Importantly, expression of $^{myc}$DGKθ completely rescued the endocytic defect in KO neurons (Figure 4B, $\tau$ $^{myc}$DGKθ = 37.0±1.1 s).

Due to the significant reduction of total DGK activity in DGKθ KO brain, we predicted that the catalytic activity of DGKθ might be essential for promoting efficient recycling of SVs. To test this hypothesis, we transiently transfected KO neurons with $^{myc}$DGKθ harboring the G648A point mutation that renders it catalytically inactive (Los et al., 2004). Consistent with our hypothesis, expression of the $^{myc}$DGKθ kinase-dead mutant ($^{myc}$DGKθ-kd) failed to rescue the delay in SV recycling kinetics in KO neurons (Figure 4B, $\tau$ $^{myc}$DGKθ-kd = 62.1±1.5 s). This was not due to the low expression or mis-targeting of the mutant as $^{myc}$DGKθ-kd expression colocalized with sypHy along neuronal processes (Figure 4C). Taken together, these data demonstrate that DGKθ catalytic activity is necessary for efficient recycling of SVs following neuronal activity.

Finally, we evaluated the effects of frequency and duration of stimuli on the rate of endocytosis. While WT neurons displayed comparable endocytic time constants across various neuronal stimuli, DGKθ KO neurons displayed a significant augmentation of the SV recycling defect with increases in the strength and frequency of neuronal stimulation (Figures 4D–4F). Thus, we conclude that during periods of sustained neuronal activity, when more APs are fired, DGKθ plays a more critical role in promoting efficient retrieval of SVs.

## Discussion

Despite speculations regarding the roles of mammalian DGKs in synaptic transmission, the function of DGKθ in the brain has remained unknown. In this study, we tested the hypothesis that DGKθ modulates neurotransmitter release at central synapses. We found that DGKθ protein expression is elevated during synaptogenesis and localizes specifically to excitatory synapses. Both acute and chronic loss of DGKθ slowed SV retrieval following neuronal stimulation. The endocytic defect could be rescued by ectopic expression of WT, but not catalytically inactive DGKθ, thus implicating DGKθ enzymatic activity in promoting the efficient recycling of SVs following neuronal activity.

A potential consequence of reduced synaptic DGK activity observed in DGKθ KO mice could be elevated levels of DAG in the plasma membrane. Since functional analogues of DAG are known to potentiate synaptic transmission (Rhee et al., 2002), we hypothesized that the slowed recycling kinetics measured in DGKθ KO neurons could be the results of augmented SV exocytosis. However, the rate of SV exocytosis reported by sypHy, assayed in the presence of the vesicular ATPase inhibitor, bafilomycin A1, was essentially identical in WT and KO neurons (Figure S2). These findings suggest that the SV recycling defect observed in DGKθ KO neurons is not secondary to altered exocytosis, and argues that DGKθ directly regulates the rate of SV endocytosis.

If DGKθ is regulating a distinct pool of DAG, not relevant for SV exocytosis, it raises the intriguing possibility that it is the PtdOH produced by DGKθ, rather than its consumption of DAG, that is crucial for maintaining efficient SV recycling. This notion is corroborated by the fact that DGKθ is responsible for generating a significant amount of PtdOH, and subsequently PtdIns in the brain. Interestingly, the role of DGKθ becomes much more prominent during intense neuronal stimulation, presumably due to an increase demand of PtdOH production at synapses. Consistent with this notion, previous studies in non-neuronal cells have shown that PtdOH production by DGKs as well as phospholipase D is important for clathrin-mediated endocytosis (Antonescu et al., 2010; Kawasaki et al., 2008; Los et al., 2004). While our data implicate a role for DGK-mediated PtdOH production in SV endocytosis at central synapses, the involvement of a PLD cannot be ruled out. A deeper understanding of the distinct mechanisms employed by individual lipid-metabolizing enzymes within the presynaptic terminal and how these pathways are integrated to ensure lipid homeostasis and efficient neuronal function will be critical for understanding the molecular basis of synaptic transmission as well as neurological diseases. Future experiments are necessary to assess physiological deficits in DGKθ KO mice as well as their behavioral phenotypes.

## Experimental Procedures

### Animals

The DGKθ KO mouse ($Dgkq^{tm1a(KOMP)Wtsi}$) was obtained from the KOMP Repository. Sprague Dawley rats were used to generate embryos for neuronal cultures. All animals were treated in accordance with the Johns Hopkins University Animal Care and Use Committee guidelines.

### Neuronal Culture and Transfection

Cortical neurons from E18 rat or E17 mouse pups were plated onto poly-L-lysine coated dishes or 18mm coverslips in Neurobasal growth medium supplemented with 2%B27, 2mM Glutamax, 50 U/mL penicillin, 50μg/mL streptomycin, and 5% Horse serum. FDU was added at *days in vitro* (DIV) 4 and neurons were maintained in glial-conditioned growth medium (1% serum) and fed twice a week. Neurons were transfected at DIV 11–12 using lipofectamine 2000 (Invitrogen) according to manufacturer's instruction. SypHy and vGlut1-pH live-cell imaging was performed DIV 14–17.

### Live-cell imaging

Coverslips containing neurons were mounted into a custom-built perfusion chamber and held at 37°C on the heated microscope stage. Cells were continuously perfused at with pre-warmed ACSF (in mM: 122.5, NaCl, 2.5 KCl, 2 $CaCl_2$, 2 $MgCl_2$, 30 D-glucose, 25 Hepes, pH 7.4) and imaged at 0.5Hz through a 40X (1.6 NA) oil objective using a Zeiss spinning-disk confocal microscope. SypHy and vGlut1-pH fluorescence was imaged at 488nm excitation and collected through a 505–550nm filter, while mCherry signal was imaged at 561nm excitation and 575–615nm emission. For KCl stimulation (ACSF with 50mM KCl, 75mM NaCl), 1μM tetrodotoxin (TTX) was added to all buffers. For field stimulation, 10μM 6-cyano-7-nitroquinoxaline-2,3-dione (CNQX) and 50μM D,L-2 amino-5-phosphonovaleric acid (AP5) were added to the ACSF instead of TTX. APs were delivered using platinum wires embedded in the imaging chamber at 100 mA and 1 ms pulse width. Quantitative imaging analyses were performed with ImageJ using the time-series plugin (Granseth et al., 2006), and the data were fitted using Prism 5 software (GraphPad Software). See Supplemental Experimental Procedures for details.

## Supplementary Material

Refer to Web version on PubMed Central for supplementary material.


## Acknowledgments

The authors thank Brian Loeper and Rebecca White for assistance in generating DGKθ KO mice; Seth Margolis, Michael Wolfgang, and members of the Huganir lab for critical discussions. This work was supported by RO1N5077923 (DMR, HLG), T32GM007445 (HLG, BCMB Training Grant), RO1N5036715 (RLH) and the John T. Reid Charitable Trusts (VA).

## References

Antonescu CN, Danuser G, Schmid SL. Phosphatidic acid plays a regulatory role in clathrin-mediated endocytosis. Mol Biol Cell. 2010; 21:2944–2952. [PubMed: 20573978]

Augustin I, Rosenmund C, Südhof TC, Brose N. Munc13-1 is essential for fusion competence of glutamatergic synaptic vesicles. Nature. 1999; 400:457–461. [PubMed: 10440375]

Balaji J, Ryan TA. Single-vesicle imaging reveals that synaptic vesicle exocytosis and endocytosis are coupled by a single stochastic mode. Proc Natl Acad Sci USa. 2007; 104:20576–20581. [PubMed: 18077369]

Bauer CS, Woolley RJ, Teschemacher AG, Seward EP. Potentiation of exocytosis by phospholipase C-coupled G-protein-coupled receptors requires the priming protein Munc13-1. J Neurosci. 2007; 27:212–219. [PubMed: 17202488]

Burger KN, Demel RA, Schmid SL, de Kruijff B. Dynamin is membrane-active: lipid insertion is induced by phosphoinositides and phosphatidic acid. Biochemistry. 2000; 39:12485–12493. [PubMed: 11015230]

Burrone J, Li Z, Murthy VN. Studying vesicle cycling in presynaptic terminals using the genetically encoded probe synaptopHluorin. Nat Protoc. 2006; 1:2970–2978. [PubMed: 17406557]

Chapman ER. How does synaptotagmin trigger neurotransmitter release? Annu Rev Biochem. 2008; 77:615–641. [PubMed: 18275379]

Cheung G, Jupp OJ, Cousin MA. Activity-dependent bulk endocytosis and clathrin-dependent endocytosis replenish specific synaptic vesicle pools in central nerve terminals. J Neurosci. 2010; 30:8151–8161. [PubMed: 20554865]

Clayton EL, Cousin MA. The molecular physiology of activity-dependent bulk endocytosis of synaptic vesicles. Journal of Neurochemistry. 2009; 111:901–914. [PubMed: 19765184]

Cremona O, Di Paolo G, Wenk MR, Lüthi A, Kim WT, Takei K, Daniell L, Nemoto Y, Shears SB, Flavell RA, et al. Essential role of phosphoinositide metabolism in synaptic vesicle recycling. Cell. 1999; 99:179–188. [PubMed: 10535736]

Di Paolo G, Moskowitz HS, Gipson K, Wenk MR, Voronov S, Obayashi M, Flavell R, Fitzsimonds RM, Ryan TA, De Camilli P. Impaired PtdIns(4,5)P2 synthesis in nerve terminals produces defects in synaptic vesicle trafficking. Nature. 2004; 431:415–422. [PubMed: 15386003]

Granseth B, Odermatt B, Royle SJ, Lagnado L. Clathrin-mediated endocytosis is the dominant mechanism of vesicle retrieval at hippocampal synapses. Neuron. 2006; 51:773–786. [PubMed: 16982422]

Haucke V, Neher E, Sigrist SJ. Protein scaffolds in the coupling of synaptic exocytosis and endocytosis. Nat Rev Neurosci. 2011; 12:127–138. [PubMed: 21304549]

Houssa B, Schaap D, van der Wal J, GOTO K, Kondo H, Yamakawa A, Shibata M, Takenawa T, van Blitterswijk WJ. Cloning of a novel human diacylglycerol kinase (DGKtheta) containing three cysteine-rich domains, a proline-rich region, and a pleckstrin homology domain with an overlapping Ras-associating domain. J Biol Chem. 1997; 272:10422–10428. [PubMed: 9099683]

Kakefuda K, Oyagi A, Ishisaka M, Tsuruma K, Shimazawa M, Yokota K, Shirai Y, Horie K, Saito N, Takeda J, et al. Diacylglycerol kinase β knockout mice exhibit lithium-sensitive behavioral abnormalities. PLoS ONE. 2010; 5:e13447. [PubMed: 20976192]

Kavalali ET. Synaptic vesicle reuse and its implications. Neuroscientist. 2006; 12:57–66. [PubMed: 16394193]

Kawasaki T, Kobayashi T, Ueyama T, Shirai Y, Saito N. Regulation of clathrin-dependent endocytosis by diacylglycerol kinase delta: importance of kinase activity and binding to AP2alpha. Biochem J. 2008; 409:471–479. [PubMed: 17880279]

Kim K, Yang J, Kim E. Diacylglycerol kinases in the regulation of dendritic spines. Journal of Neurochemistry. 2010; 112:577–587. [PubMed: 19922438]

Kononenko NL, Haucke V. Molecular mechanisms of presynaptic membrane retrieval and synaptic vesicle reformation. Neuron. 2015; 85:484–496. [PubMed: 25654254]

Los AP, van Baal J, de Widt J, Divecha N, van Blitterswijk WJ. Structure-activity relationship of diacylglycerol kinase theta. Biochim Biophys Acta. 2004; 1636:169–174. [PubMed: 15164764]

Luo B, Prescott SM, Topham MK. Diacylglycerol kinase zeta regulates phosphatidylinositol 4-phosphate 5-kinase Ialpha by a novel mechanism. Cell Signal. 2004; 16:891–897. [PubMed: 15157668]

Mani M, Lee SY, Lucast L, Cremona O, Di Paolo G, De Camilli P, Ryan TA. The Dual Phosphatase Activity of Synaptojanin1 Is Required for Both Efficient Synaptic Vesicle Endocytosis and Reavailability at Nerve Terminals. Neuron. 2007; 56:1004–1018. [PubMed: 18093523]

McMullan R, Hiley E, Morrison P, Nurrish SJ. Rho is a presynaptic activator of neurotransmitter release at pre-existing synapses in *C. elegans*. Genes Dev. 2006; 20:65–76. [PubMed: 16391233]

Mérida I, Avila-Flores A, Merino E. Diacylglycerol kinases: at the hub of cell signalling. Biochem J. 2008; 409:1–18. [PubMed: 18062770]

Musto A, Bazan NG. Diacylglycerol kinase epsilon modulates rapid kindling epileptogenesis. Epilepsia. 2006; 47:267–276. [PubMed: 16499750]

Nurrish S, Ségalat L, Kaplan JM. Serotonin inhibition of synaptic transmission: Galpha(0) decreases the abundance of UNC-13 at release sites. Neuron. 1999; 24:231–242. [PubMed: 10677040]

Puchkov D, Haucke V. Greasing the synaptic vesicle cycle by membrane lipids. Trends in Cell Biology. 2013; 23:493–503. [PubMed: 23756446]

Rhee JS, Betz A, Pyott S, Reim K, Varoqueaux F, Augustin I, Hesse D, Südhof TC, Takahashi M, Rosenmund C, et al. Beta phorbol ester- and diacylglycerol-induced augmentation of transmitter release is mediated by Munc13s and not by PKCs. Cell. 2002; 108:121–133. [PubMed: 11792326]

Rohrbough J, Broadie K. Lipid regulation of the synaptic vesicle cycle. Nat Rev Neurosci. 2005; 6:139–150. [PubMed: 15685219]

Shirai Y, Kouzuki T, Kakefuda K, Moriguchi S, Oyagi A, Horie K, Morita SY, Shimazawa M, Fukunaga K, Takeda J, et al. Essential role of neuron-enriched diacylglycerol kinase (DGK), DGKbeta in neurite spine formation, contributing to cognitive function. PLoS ONE. 2010; 5:e11602. [PubMed: 20657643]

Südhof TC. The synaptic vesicle cycle. Annu Rev Neurosci. 2004; 27:509–547. [PubMed: 15217342]

Tu-Sekine B, Raben DM. Regulation and roles of neuronal diacylglycerol kinases: a lipid perspective. Critical Reviews in Biochemistry and Molecular Biology. 2011; 46:353–364. [PubMed: 21539478]

Tu-Sekine B, Raben DM. Dual regulation of diacylglycerol kinase (DGK)-θ: polybasic proteins promote activation by phospholipids and increase substrate affinity. Journal of Biological Chemistry. 2012; 287:41619–41627. [PubMed: 23091060]

Ueda S, Tu-Sekine B, Yamanoue M, Raben DM, Shirai Y. The expression of diacylglycerol kinase theta during the organogenesis of mouse embryos. BMC Dev Biol. 2013; 13:35. [PubMed: 24079595]

Watanabe S, Rost BR, Camacho-Pérez M, Davis MW, Söhl-Kielczynski B, Rosenmund C, Jorgensen EM. Ultrafast endocytosis at mouse hippocampal synapses. Nature. 2013; 504:242–247. [PubMed: 24305055]

Wu Y, O'Toole ET, Girard M, Ritter B, Messa M, Liu X, McPherson PS, Ferguson SM, De Camilli P. A dynamin 1-, dynamin 3- and clathrin-independent pathway of synaptic vesicle recycling mediated by bulk endocytosis. eLife. 2014; 3:e01621. [PubMed: 24963135]

Yang J, Seo J, Nair R, Han S, Jang S, Kim K, Han K, Paik SK, Choi J, Lee S, et al. DGKι regulates presynaptic release during mGluR-dependent LTD. The EMBO Journal. 2011; 30:165–180. [PubMed: 21119615]

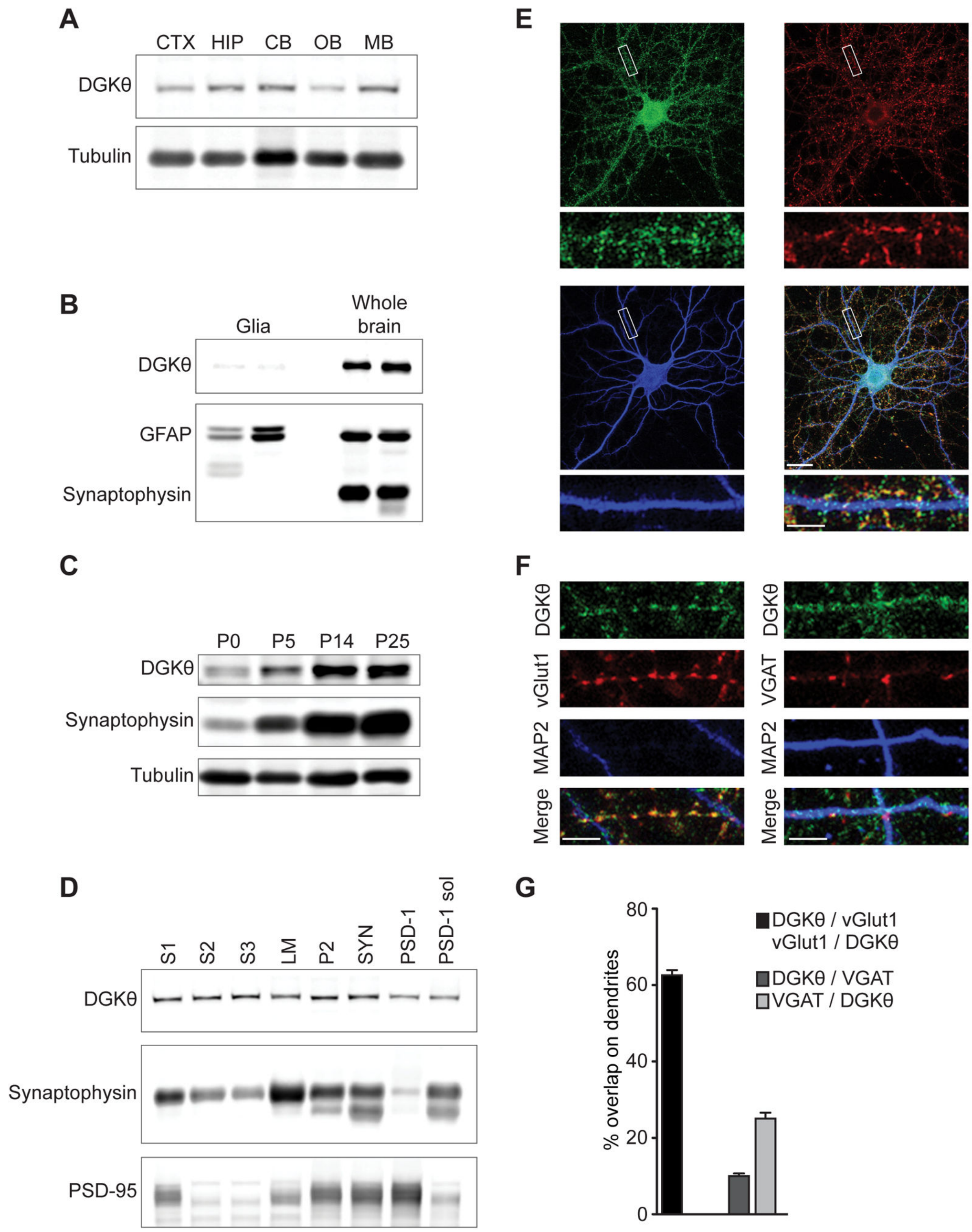


**Figure 1. DGKθ is an excitatory synaptic protein**

**A)** Protein extracts prepared from adult mouse cortex (CTX), hippocampus (HIP), cerebellum (CB), olfactory bulb (OB), and midbrain (MB) were assayed for DGKθ protein expression by western blot using specific antibodies against DGKθ and tubulin (loading control).

**B)** Whole-cell extracts from primary glial cultures and rat whole brain were blotted with specific antibodies against DGKθ, GFAP (glial marker), and synaptophysin (neuronal marker).

**C)** Whole brain lysates from mice between postnatal day 0 (P0) and 25 (P25) were assayed for DGKθ protein expression by using antibodies against DGKθ, synaptophysin, and tubulin.

**D)** Biochemical fractionation of adult mouse brain reveals a wide distribution of DGKθ in various subcellular compartments. Synaptophysin and PSD-95 (pre- and postsynaptic protein markers, respectively) were used as controls for successful isolation of synaptic fractions. Post-nuclear supernatant (S1), cytosol after P2 precipitation (S2), cytosol after LM precipitation (S3), light membranes (LM), crude synaptosomes/membranes (P2), synaptosomes (SYN), postsynaptic density (PSD-I), remaining soluble fraction after PSD-I precipitation (PSD-I sol). 20μg of protein was loaded for each fraction.

**E–F**) Cultured hippocampal neurons (DIV28) were immunostained with specific antibodies against DGKθ, vGlut1 (excitatory presynaptic protein) or VGAT (inhibitory synaptic marker) and MAP2 (dendritic protein). Scale bar, 20μm and 5μm (crop region).

**G)** Quantification of the average overlap between DGKθ/vGlut1 and DGKθ/VGAT staining on MAP2-positive secondary dendrites. Data represent mean ± SEM (n = 3 independent coverslips).

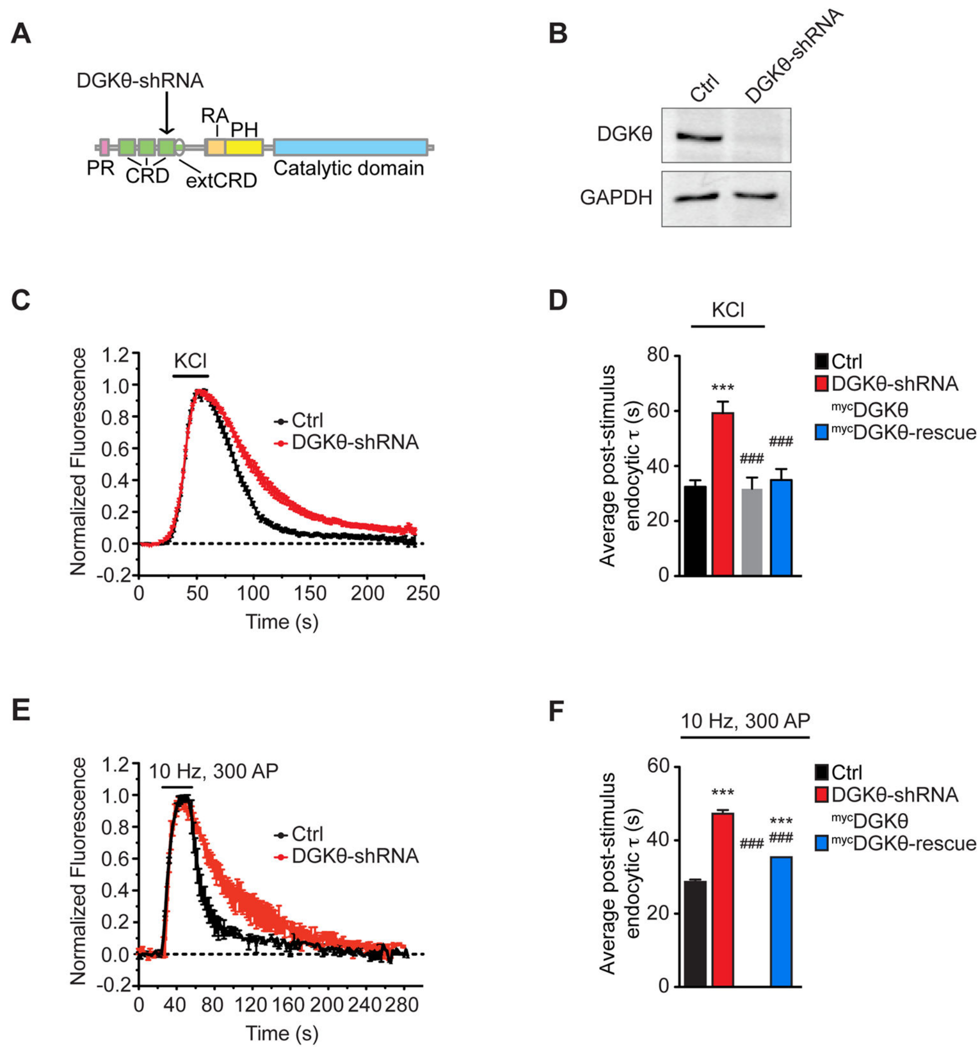


**Figure 2. DGKθ regulates the kinetics of SV recycling in cortical neurons**

**A)** Schematic of the domain structure of DGKθ and the relative location of the DGKθ-shRNA target.

**B)** Lysates from cultured cortical neurons infected with either control (Ctrl) or DGKθ-shRNA lentivirus were subjected to western blot analysis with antibodies against DGKθ and GAPDH (loading control).

**C)** Normalized average traces from neurons expressing sypHy with either control (black) or DGKθ-shRNA (red) in response to 60s stimulation with high $K^+$ buffer.

**D)** Comparison of average τ values between control and DGKθ-shRNA from (**C**), $^{myc}$DGKθ (+ctrl shRNA, grey), and $^{myc}$DGKθ-rescue (green) neurons. The decay phases of the traces were fitted with single exponential functions and τ values were calculated from the fits.

**E)** Normalized average traces from neurons expressing sypHy with control or DGKθ-shRNA in response to a train of 300 APs (10Hz).

**F)** Comparison of average τ values between control and DGKθ-shRNA from (**E**), $^{myc}$DGKθ and $^{myc}$DGKθ-rescue neurons in response to the 10Hz stimulus.

For all experiments shown in Figure 2, data represent mean ± SEM from ≥100 boutons; *** P<0.001 against Ctrl; ### P<0.001 against DGKθ-shRNA, a one-way analysis of variance (ANOVA) with Tukey's *post-hoc* test.

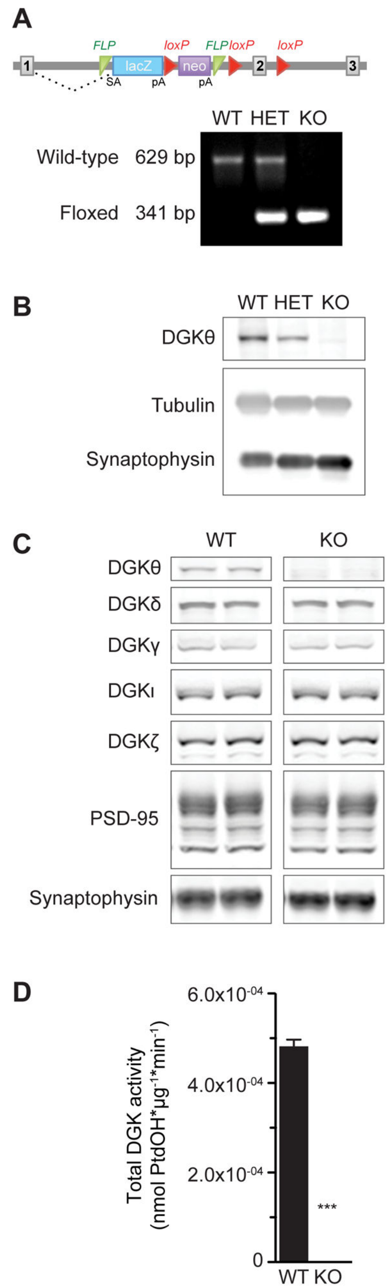


**Figure 3. Total DGK activity is reduced in DGKθ KO mice**

**A)** Top, schematic of DGKθ knock-out allele (Dgkq$^{tm1a(KOMP)Wtsi}$). Exon 1 is spliced to the artificial splice acceptor (SA) in front of lacZ instead of another exon in the DGKθ gene. The poly-adenylation site (pA) terminates transcription after lacZ, preventing the transcription of the DGKθ RNA. Bottom, typical result of PCR for genotyping. Bands at 629bp and 341bp areindicative of DGKθ WT and KO alleles, respectively.

**B)** Western blot analysis of protein extracts prepared from DGKθ WT, HET and KO mouse brain tissue confirms the loss of DGKθ protein in KO lysates. Tubulin and synaptophysin blot showed equal loading of protein lysates.

**C)** Western blot analysis of brain tissue isolated from 2 pairs of WT and KO mice run on the same gel. Samples were immunoblotted with antibodies against DGKθ, −γ, −ι, −ζ, representing 4 classes of DGKs. Synaptophysin and PSD-95 blots showed equal loading of protein lysates.

**D)** Average total DGK activity measured *in vitro* in 5μg of S1 fractions from 5 pairs of age-matched WT and KO forebrain tissues. Averages include 3 technical replicates per sample. Error bars represent SEM. Student's t test, *** P<0.0001 against WT.

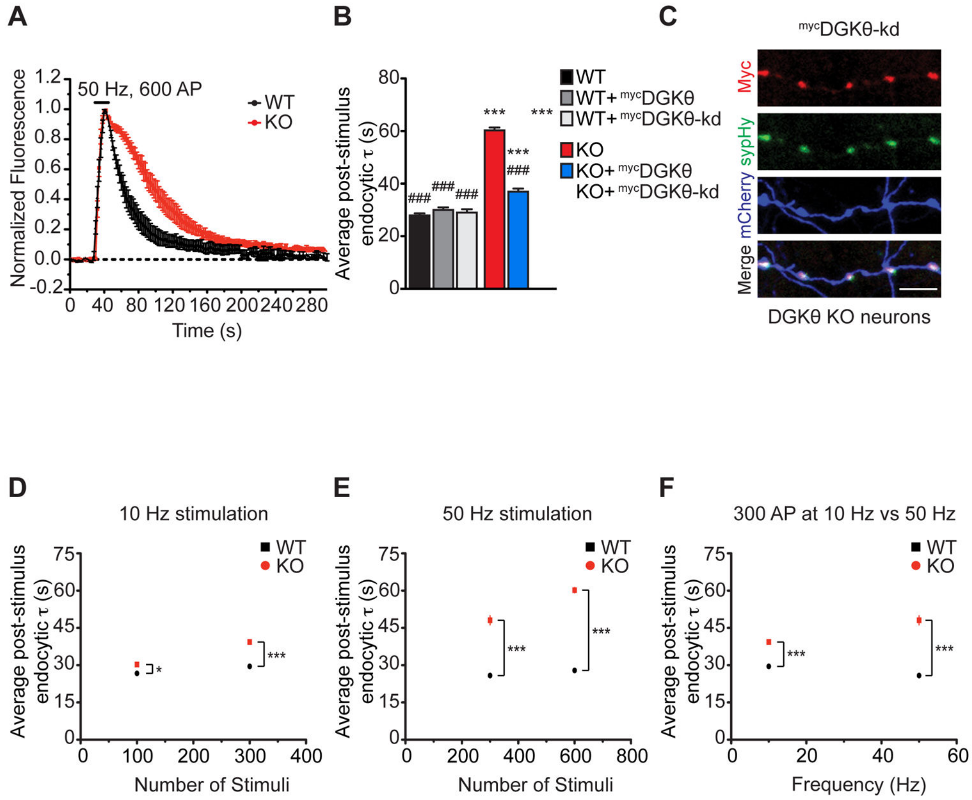


**Figure 4. DGKθ enzymatic activity is required for efficient SV recycling**

**A)** Normalized average traces from WT (black) and KO (red) neurons expressing sypHy in response to a train of 600 APs (50Hz).

**B)** Comparison of average $\tau_{endo}$ values between WT and KO neurons expressing empty vector from (**A**), mycDGKθ, or kinase-dead DGKθ (mycDGKθ-kd) in response the 50Hz stimulus.

**C)** DGKθ KO neurons (DIV20) expressing sypHy, mCherry, mycDGKθ-kd were stained with anti-myc (red), anti-GFP (green), and anti-mCherry (blue) antibodies. Merge panel (bottom) shows mycDGKθ-kd colocalizes with sypHy reporter. Scale bar, 5μm.

**D–F**) Defect in SV recycling is exaggerated with increasing number of stimuli (**D–E**) and higher frequency stimulation (**F**).

**D)** Average τ values measured in WT and KO neurons following trains of 100 or 300 APs delivered at 10Hz.

**E)** Average τ values measured in WT and KO neurons following trains of 300 or 600 APs delivered at 50Hz.

**F)** Comparison of the average τ values from (**D–E**) following a train of 300 APs delivered at 10Hz and 50Hz.

For all experiments shown in Figure 4, data represent ± SEM from ≥200 boutons per condition; *** P < 0.001, against WT, ### P<0.001 against KO, ANOVA with Tukey's *post-hoc* test.